

Lawrence Berkeley National Laboratory

Recent Work

Title

CALORIMETRIC STUDIES OF SINGLET-GROUND-STATE SYSTEMS

Permalink

<https://escholarship.org/uc/item/5pv443w2>

Author

Wun, Marilyn.

Publication Date

1974-09-01

00004201660

LBL-3177

c.1

SEP 1974

CALORIMETRIC STUDIES OF SINGLET-GROUND-STATE SYSTEMS

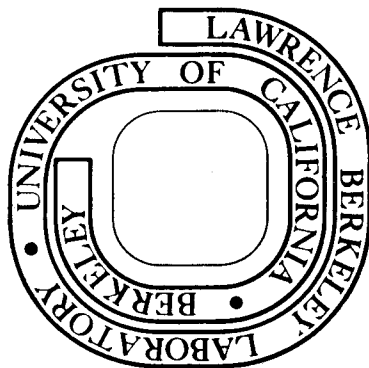
Marilyn Wun
(M.S. thesis)

September, 1974

Prepared for the U. S. Atomic Energy Commission
under Contract W-7405-ENG-48

For Reference

Not to be taken from this room



LBL-3177
c.1

DISCLAIMER

This document was prepared as an account of work sponsored by the United States Government. While this document is believed to contain correct information, neither the United States Government nor any agency thereof, nor the Regents of the University of California, nor any of their employees, makes any warranty, express or implied, or assumes any legal responsibility for the accuracy, completeness, or usefulness of any information, apparatus, product, or process disclosed, or represents that its use would not infringe privately owned rights. Reference herein to any specific commercial product, process, or service by its trade name, trademark, manufacturer, or otherwise, does not necessarily constitute or imply its endorsement, recommendation, or favoring by the United States Government or any agency thereof, or the Regents of the University of California. The views and opinions of authors expressed herein do not necessarily state or reflect those of the United States Government or any agency thereof or the Regents of the University of California.

CALORIMETRIC STUDIES OF SINGLET-GROUND-STATE SYSTEMS

Contents

ABSTRACT	v
I. INTRODUCTION	1
II. PrCu_2	3
III. TERBIUM ETHYL SULFATE	8
APPENDIX I. EXPERIMENTAL TECHNIQUES	12
A. Apparatus for the Temperature Range from 0.06K to 1K	12
B. Apparatus for the Temperature Range from 0.3K to 20K	13
C. Sample Holders (Adaptors)	13
D. Heat Capacity Calculations	14
E. Heat Capacity of the Addenda	14
APPENDIX II. THE HEAT CAPACITY OF APIEZON-N GREASE	17
APPENDIX III. THE HEAT CAPACITY OF LaCu_2	20
APPENDIX IV. DATA SHEETS	21
REFERENCES	39
ACKNOWLEDGEMENTS	41
TABLES	42
FIGURE CAPTIONS	44
FIGURES	45

CALORIMETRIC STUDIES OF SINGLET-GROUND-STATE SYSTEMS

Marilyn Wun

Inorganic Materials Research Division, Lawrence Berkeley Laboratory
and Department of Chemistry; University of California,
Berkeley, California

ABSTRACT

Terbium ethyl sulfate and PrCu_2 are examples of compounds in which the rare earth ions are in singlet crystal field ground states and the exchange coupling between ions is smaller than the critical value required for magnetic moment formation. Heat capacity measurements on PrCu_2 suggest that the singlet ground state arises from a Jahn-Teller distortion and give a value for the hyperfine enhancement of magnetic field at the nucleus. In terbium ethyl sulfate a cooperative transition to an ordered state is observed at 0.25 K. This transition probably arises from a combination of dipole-dipole and hyperfine interactions.

I. INTRODUCTION

For a rare earth ion usually only one J multiplet is populated at room temperature and below, and the ion has a magnetic moment determined by J and g . Crystalline electric fields can split the $2J+1$ levels of the multiplet, and if the ion has an even number of electrons, it is possible for the ground level to be a non-magnetic singlet. In such a case magnetic moments can occur in the low temperature limit only if some perturbation such as an external field or an exchange coupling between the ions mixes higher states with the ground state. The former case is known as Van Vleck paramagnetism. In the latter case there is a critical value of the ratio of J , the exchange coupling parameter, to Δ , the crystal field splitting, required for the appearance of magnetic moments.

If the calculated susceptibility including crystal-field effects but not exchange coupling is χ , and the exchange effects are represented by a molecular field approximation (MFA) with λ the molecular field parameter, the observed susceptibility is $\chi = \chi'/(1-\lambda\chi')$.¹ For the special case of two singlet levels separated by an energy $k\Delta$ magnetic moments occur only if $\lambda\chi'_0 > 1$ where χ'_0 is the 0K value of χ' , and the critical temperature below which moments appear is given by the solution of $\chi'/\chi'_0 = \tanh(\Delta/2kT)$.¹

These singlet ground state systems have attracted attention for several reasons: They constitute a class of systems showing cooperative magnetic transitions and provide examples for testing theories of cooperative ordering. They have also been recognized as potentially

useful in the production of low temperatures by adiabatic nuclear demagnetization because the effective field at the nucleus is greater than the applied field. The enhancement arises from the hyperfine coupling of the nuclear moment to the Van Vleck electronic moment and is usually represented by a factor $1+K$ where K is determined by the Van Vleck paramagnetic susceptibility and the hyperfine coupling.

In this thesis calorimetric investigations of two singlet ground state systems are reported. In terbium ethyl sulfate the two lowest crystal field levels are singlets and all other levels are appreciably higher. The magnitude of J is too small to produce magnetic moments but both the hyperfine coupling and the dipole-dipole coupling are comparable with Δ and, apparently, one or the other or a combination of the two produces moments.² In PrCu_2 J is also less than the critical value for the formation of electronic moments, but a cooperative nuclear ordering has been reported.³ Presumably it arises from a nuclear-nuclear interaction enhanced by the hyperfine coupling of the nucleus to the electrons and the (subcritical) exchange coupling between ions.

II. PrCu_2

Andres et al.³ found a heat capacity anomaly in PrCu_2 that had a maximum around 7K and an entropy close to $R\ln 2$. Nearly temperature-independent susceptibility between 1 and 7K rules out the possibility of the anomaly being a precursor to magnetic order and suggests that the ground state is a singlet. They interpreted the anomaly as originating from a first excited singlet state which is separated in energy from the ground crystal field state by $k \times 13\text{K}$. They found the heat capacity of PrCu_2 below 0.5K increased with decreasing temperatures. Below 90mK they found a faster than $1/T^2$ dependence where a normal hyperfine heat capacity would have a $1/T^2$ dependence. Their susceptibility measurements show a maximum at 54mK in 110 Oe. The behavior of the heat capacity and the susceptibility together were interpreted as associated with a cooperative antiferromagnetic nuclear ordering.

The original PrCu_2 sample used in our measurements, sample I, was prepared by melting the components in an arc furnace. The components consisted of 40.0185 gms of 99.9% pure Pr metal and 35.8734 gms of a 99.999% pure Asarco copper rod. The sample was in the shape of a right circular cylinder about 3/4 in. in diameter and 1 in. long. X-ray examination of sample I showed only the PrCu_2 phase. The heat capacity of this sample was measured in zero field from 0.3 to 20K. After that run, the sample cracked and the following measurements were made on a fragment, sample II, from the lower portion of the original sample. Chemical analysis on a part of sample II gave 51.90% by weight of Pr and 48.28% by weight of Cu. The heat capacities of

samples I and II were different below 3.2K, but indistinguishable between that temperature and 8K. In the following, it has been assumed that samples I and II have the same heat capacity above 3.2K. Sample II was measured in zero field from 0.06 to 20K, in 9 kOe from 0.13 to 0.4K, in 10 kOe from 0.3 to 0.6K, in 20 kOe from 0.3 to 0.6 K, and in 38 kOe from 0.38 to 20K. Sample III was prepared by remelting and annealing sample II. The sample was held at 900-910°C for 45 min. Then at 835-840°C for 45 min and at 800-820°C for three days, all under vacuum. Sample III was measured only in zero field below 0.63K and had a heat capacity on the order of 20% higher than sample II. Heat capacities were measured as described in Appendix I.

Figures 1 and 2 show the 7K anomaly. The data in these figures except for some of the high temperature zero field points which were taken on sample I are all on sample II. They also include the heat capacity of LaCu_2 used to provide a rough estimate of the electronic and lattice heat capacities of PrCu_2 . (See Appendix III for details.) The zero field 7K anomaly is approximately 25% higher than that reported by Andres et al. and somewhat sharper. The anomaly is much sharper than a Schottky for a two-level system as shown in Fig. 2, but similar to anomalies which have been observed for TmVO_4 ⁴ and TmAsO_4 ⁵ and interpreted as arising from a Jahn-Teller distortion. (The Jahn-Teller effect is a distortion of the lattice that lifts the degeneracy of the two degenerate or nearly degenerate levels and produces, at low temperatures, a lowering of the crystal field energy.) The anomalies for these compounds are quite accurately reproduced by a

molecular field calculation. Our results show a broader transition than would be obtained by a molecular field calculation. This presumably is the result of inhomogeneities in the sample. The solid curve in Fig. 2 represents a molecular field calculation for a doublet ground state broadened by a gaussian distribution of critical temperatures with $\bar{T}_D = 7.5\text{K}$ and the half width in critical temperature, $\delta T_D = 0.35\text{K}$ to account for the inhomogeneities. The sum of the molecular field calculation and the heat capacity of LaCu_2 does not account for all of the heat capacity of PrCu_2 near 8K and above. The additional substantial heat capacity at these temperatures is most likely due to a Schottky anomaly peaking around 12 or 13K. This Schottky anomaly is probably the result of a third crystal field state near 25K. Thus, although we have not made a detailed calculation, it seems probably that the crystal field heat capacity in the 1 to 20K region is the sum of a cooperative Jahn-Teller distortion involving the two lowest singlet states (which have a separation much smaller than 7K at high temperatures) and a third state near 25K (which may also be affected by the distortion). This interpretation is different from that of Andres et al., but is still consistent with the Pr ions in PrCu_2 being in a singlet ground state at temperatures small compared with 7K.

Our heat capacity results below 1K for PrCu_2 in zero applied field and several magnetic fields are shown in Fig. 3. In this region, our results (on sample II) and those reported by Andres et al. have a slightly different temperature dependence. They report a faster than $1/T^2$ dependence below about 90 mK whereas our results show a slower than a $1/T^2$ dependence above 80 mK while the few points below 80 mK

increase as rapidly as $1/T^2$. Furthermore, our heat capacity results are lower than theirs--only 70% at high as 0.1K. (Although our results on sample III are higher than that on sample II, they are still substantially lower than that of Andres et al.) For $0.3 \leq T \leq 0.6K$ and $0 \leq H \leq 20$ kOe the data are approximately represented by

$$C = 0.029T + (0.003 + 7.94 \times 10^{-5} H^2)T^{-2} \text{ J/mole-K,}$$

where H is the magnetic field in kOe. The heat capacity increases in a magnetic field as one would expect for a singlet ground state. In this region of temperature and magnetic field the field dependent term can only be a hyperfine enhanced nuclear contribution,

$$C/R = \frac{1}{3} \frac{(I+1)}{I} (1+K)^2 \left(\frac{\mu H}{kT}\right)^2.$$

We find for $1+K$, the factor by which the applied field is enhanced at the nucleus, $1+K = 29$. This value is in reasonable agreement with that obtained by Andres et al. from their analysis of nuclear magnetic susceptibilities below 0.5K.

In summary, our interpretation of the crystal field heat capacity is substantially different from that given by Andres et al. but still corresponds to a singlet ground state of the Pr^{+3} ions in PrCu_2 . The field dependence of the heat capacity at moderately low temperatures gives an enhancement factor in reasonable agreement with their value and therefore supports their interpretation of the susceptibility at temperatures just above the maximum. Our heat capacity measurements show no indication of a cooperative anomaly, but they do not extend to the temperature of the susceptibility maximum. However, the sample dependence of the low temperature heat capacity suggest the possibility

0 0 0 0 4 2 0 1 6 6 5

-7-

that it is associated with a minor constituent. Obviously, measurements on a more perfect sample would be of interest.

III. TERBIUM ETHYL SULFATE

The two lowest energy levels of the Tb^{+3} ion in terbium ethyl sulfate are singlets separated by 0.4 cm^{-1} .⁶ An EPR study of Tb-Tb pairs in YES has shown⁷ that the only interaction of significance between Tb^{3+} ions is the dipole-dipole one. Susceptibility measurements show ferromagnetic ordering around $0.24K$.² For nearest neighbors along the c-axis the dipole-dipole energy corresponds approximately to $0.25K$ and it has been suggested that terbium ethyl sulfate is an example of a system where formation of the magnetic moments is produced by dipole-dipole coupling.² However, the hyperfine coupling constant is $A = 0.30K$ (where $AS_z I_z$ is the hyperfine term in the Hamiltonian) so the possibility that the hyperfine term is important in moment formation cannot be ruled out.

The heat capacity of terbium ethyl sulfate was measured between 70 mK and $20K$, but at temperatures below $0.13K$ the sample shows extremely long relaxation times--on the order of several hours. Above $0.13K$ the relaxation times were less than 10 min . The long relaxation times cannot be handled with our experimental setup. Because of the uncertainty that these relaxation times introduce we report only the results above $0.15K$. The heat capacity measurements were made as described in Appendix I. (See Appendix II for details on the Apiezon N grease used as a thermal bonding agent.)

A considerable complication in the data is associated with an apparent sensitivity of the heat capacity to the loss of water of hydration. This effect appeared as successive decreases in the heat

of the first sample from run to run. It was concluded that this effect was associated with the loss of water of hydration when exposed to the insulating vacuum of the calorimeter before cooling or when warming to room temperature. A second sample was obtained and care was taken not to expose it to the insulating vacuum. However, problems with the He³ apparatus delayed measurements in the 0.3 to 20K region for several months. During that period the sample was cooled to 77K several times and warmed back to room temperature. After a successful experiment was finally carried out, the data was found to be about 2% lower than the adiabatic data (0.15K to 0.5K range) in the overlap range even though the above precautions had been taken.

We believe that the low temperature measurements on the second sample give correctly the heat capacity below 0.5K. Measurements on the first sample show that the loss of water of hydration has an effect at all temperatures. As an approximate correction to the high temperature data on the second sample we have scaled up the $1/T^2$ term (see following description of analysis) by 2% so that the two sets of data meet.

In the temperature region between 2 and 3.6K the data are represented by

$$C = 1.7560/T^2 + 0.00649T^3 \text{ J/mole-K}$$

but in accord with the above mentioned approximation, we have used

$$C = 1.79112/T^2 + 0.00649T^3 \text{ J/mole-K.}$$

This allows us to separate the data into two contributions, the magnetic heat capacity C_M and the lattice heat capacity C_L . Below 2K the magnetic heat capacity $C_M = C - 0.00649T^3$ J/mole-K. Above 2K, $C_M = 1.79112/T^2$ J/mole-K. Below 2K the lattice heat capacity

$$C_L = 0.00649T^3 \text{ J/mole-K. Above 2K } C_L = C - 1.79112/T^2 \text{ J/mole-K.}$$

The results of this analysis are shown in Figs. 4 and 5 as $(C - 0.00649T^3)$ vs T and $(C - 1.79112/T^2)/T^3$ vs T , respectively. Table I gives values of $(C - 1.79112/T^2)/T^3$ from Fig. 5 at one degree intervals. Comparison of our results for C_L with the results reported by Meyer and Smith⁸ on several other rare-earth ethylsulfates show reasonable agreement. The shape of the curve above 2K and the position of the peak in Fig. 5 are very similar to that of Meyer and Smith's. We have attributed the upturn in C/T^3 reported by these authors even in non-magnetic rare-earth ethylsulfates as an experimental error associated with the use of helium exchange gas. At 9K they give a lattice heat capacity value of 9.84 mJ/mole-K for ytterbium ethyl sulfate and neodymium ethyl sulfate⁸ which is in close agreement with our results of 9.875 mJ/mole-K at the same temperature.

The magnetic heat capacity shown in Fig. 4 is consistent with known crystal field splittings and the previously reported susceptibility. A sharp peak of the kind typically associated with a cooperative transition is superimposed on the low temperature side of a broader Schottky-like anomaly that occurs at the temperature expected from the crystal field splitting.

The total entropy associated with the magnetic heat capacity above 0.13K (using a $1/T^2$ extrapolation above 2K to $T = \infty$) is 10.19 J/mole-K which is substantially more than $R \ln 2 = 5.763$ J/mole-K expected for the two crystal field levels alone. This is not particularly surprising because the formation of magnetic moments at 0.25K, the approximate

temperature of the cooperative transition observed in both the heat capacity and the susceptibility, would produce a substantial hyperfine field and the nuclear heat capacity should be quite appreciable at that temperature and below. What is somewhat surprising, however, is that the entropy above 0.25K is very close to $R\ln 2$. If it is assumed that some of the entropy below 0.25K is associated with the formation of electronic moments and therefore part of the $R\ln 2$ entropy arising from the two crystal field levels, it follows that some of the entropy above 0.25K must be nuclear in origin. This suggests that the hyperfine coupling has some role in the production of electronic moments and that the formation of these moments takes place partially above 0.25K, but in the absence of a detailed theoretical calculation this is speculative.

In summary, the heat capacity measurements have confirmed the occurrence of cooperative ordering at 0.25K. There is some indication that the hyperfine coupling is important in this transition but a firm conclusion must await further theoretical developments.

APPENDIX I. EXPERIMENTAL TECHNIQUES

Two methods of cooling were used, magnetic cooling (adiabatic demagnetization apparatus) and He³ refrigeration (He³ apparatus). The apparatus will be described in the following two sections.

A. Apparatus for the Temperature range from 0.06K to 1K

The adiabatic demagnetization cryostat used for measurements in the 0.06K to 1 K range is described by Triplett.⁹

By potentiometrically monitoring a germanium resistance thermometer (GE1751) thermally anchored to the calorimeter, temperature drifts between heat capacity points (taken via the heat pulse technique) and rises in temperature during heat capacity points were recorded. The germanium thermometer (GE1751) was calibrated on the laboratory's temperature scale designated T_η. For details on thermometer and thermometer calibrations the reader is referred to the Ph.D. theses of Bader¹⁰ and Conway.¹¹

The calorimeter made of high-purity silver ends in a threaded bobbin to which a tapped sample or tapped sample holder (adaptor) can be mounted. Thermal contact between the sample and the calorimeter is made through the threads of the bobbin.

A superconducting high-purity lead wire is used to make and break thermal contact between the cooling salt and the calorimeter. For details on calorimeter design and experimental technique see Triplett's⁹ and Bader's¹⁰ Ph.D. theses.

B. Apparatus for the Temperature Range from 0.3K to 20K

For measurements in the 0.3K to 20K range He³ refrigeration was used to cool the samples. The He³ cryostat is described in references 10 and 9.

Here the calorimeter is made of copper and, instead of a lead switch, a mechanical heat switch is used to make thermal contact between the calorimeter and the pumped He³ used for refrigeration. A germanium resistance thermometer (Ge1609) is thermally anchored to the calorimeter to monitor the temperature of the sample. It is also calibrated on the T_η temperature scale. (See Triplett's and Bader's Ph.D. theses.^{9,10})

C. Sample Holders (Adaptors)

In the case of the Apiezon N grease a small cup-like adaptor was fabricated out of three thin cylinders of copper concentrically situated on and hard soldered to a thin circular copper plate. A piece of copper wire connected the tapped portion of the adaptor to the cup portion. The entire sample holder was then plated with approximately 0.5 mil thickness of gold. The adaptor was then measured to determine its heat capacity.

The adaptor for the PrCu₂ was machined from a rod of "as-received" 6-9's Cominco silver to which a piece of silver foil was joined with milligram quantities of hard-solder. The adaptor was not measured but assumed to be pure silver. It's heat capacity will be discussed in section E.

A cell made from high-purity copper was used for the terbium ethyl sulfate experiments. One end of the cell was tapped so it could be

mounted on the calorimeter. The other end was open and had threads on which the bottom tapped plate could be mounted. Inside the cell small amounts of hard-solder were used to attach small copper fins for better thermal contact to the sample. The sample was packed in the cell and the bottom plate mounted. The cell was not measured but assumed to be pure copper. Its heat capacity will be discussed in section E.

D. Heat Capacity Calculations

The heat capacity of a sample is given by

$$C = (C_{\text{Total}} - C_{\text{Addenda}})/n$$

where C_{Total} is the total measured heat capacity, C_{Addenda} is the sum of the heat capacity of the empty calorimeter, an adaptor (if there is one), and of any thermal bonding agents used, and n is the number of moles or grams of sample (depending on whether it is more convenient to have the sample on a per mole basis or per gram basis). The heat capacity contributions of the addenda will now be discussed separately.

E. Heat Capacity of the Addenda

The heat capacity of the empty copper calorimeter is given by

$$C_{\text{MT}} = C_c (1 + \Delta(T, H))$$

where

$$C_c = \frac{A(H)}{T^2} + \sum_{i=1}^6 B_i T^{b_i}, \quad b_i = 1, 2, 3, 5, 7, \text{ and } 9.$$

A was determined graphically and the B_i coefficients were determined by a least squares fit to the data after the $A(H)/T^2$ term was subtracted. The coefficient of the $1/T^2$ term was found to be a function of the

applied field, H, so $\Delta(T,H)$ is also a function of field. (See ref. 10.) A Δ -table was constructed by reading values of Δ at intervals of $\log_{10} T(K)$ from a smooth curve drawn through a graph of the fractional differences $[\Delta(T)]$ between the sample heat capacities, C , and C_c as a function of the logarithm of the temperature. Interpolations done on this Δ -table give the desired $\Delta(T)$ values.

The heat capacity of the copper sample holder is

$$C_{\text{Adaptor}} = C'_c [1 + \Delta(T)]$$

$$\text{where } C'_c = \sum_{i=0}^3 B_{2i+1} T^{2i+1}.$$

The coefficients, B_{2i+1} , were determined by a least squares fit to the data. A Δ -table for the adaptor was constructed in the same manner as discussed above.

The heat capacity of the silver adaptor was calculated from

$$C_{\text{Ag}} = \left[\sum_{i=0}^4 B_i T^{2i+1} \right] \cdot X$$

which was obtained by least-squares fitting to (a) the smoothed data for $1 \leq T \leq 5$ K generated from Ahler's equation¹² and multiplied by the factor 0.994 to join Martin's data in the overlap region and (b) Martin's¹³ smoothed data for $3 \leq T \leq 30$ K. A Δ -table was not constructed from the fractional differences to improve the determination of C_{Ag} as this would probably reflect Martin's temperature scale which most likely is slightly different from that used here. The weight of the adaptor in terms of the number of moles was used for X. (The coefficients of the equation are on a per mole of Ag basis.)

The heat capacity of the copper cell was calculated from

$$C_{\text{Cu}} = [\gamma T + \sum_{i=1}^3 B_i T^{2i+1}] (1 + \Delta(T)) \cdot Y$$

which was obtained by least-squares fitting of data taken on a rod of high-purity Asarco copper which had been annealed and then melted. (See Triplett's Ph.D. thesis for details on the Asarco rod.) For Y, the number of moles of copper, the weight of the copper cell was used, ignoring milligram quantities of hard solder. The value of γ was determined graphically and the B_i coefficients were determined by least-squares fitting of the data after the γT term had been subtracted. This forces the fractional differences at the low temperature end to go to zero. The data on the Asarco rod covered the region from 0.3K to 20K. This method allows one to use just the determined equation (i.e. no Δ -table) in regions below 0.3K. A Δ -table was constructed in the same manner as discussed above.

The equation:

$$C_{\text{GE7031}} = \left[\sum_{i=1}^8 A_i T^i \right] \cdot \left[1 + \Delta(T) \right] \cdot Z$$

was used in the LaCu_2 analysis but in the PrCu_2 analysis the approximately 50 milligram quantities of GE7031 varnish used contributed a negligible amount to the heat capacity so it was not corrected for. For Z the number of grams of GE7031 used was entered. For details on the origin of this equation see Bader's Ph.D. thesis.¹⁰

APPENDIX II. THE HEAT CAPACITY OF APIEZON-N GREASE

Apiezon grease is frequently used to make thermal contact at cryogenic temperatures. However, the addition of the thermal bonding agent contributes to the total heat capacity measured. To get a more accurate picture of the heat capacity of the system, the contribution due to the grease must be subtracted. To facilitate this, the specific heat of Apiezon-N grease was measured in the temperature region from 0.4K to 20K and, subsequently, fitted to a polynomial in powers of temperature, $T(K)$, by a least-squares method.

The measurement on the Apiezon N grease was carried out in the He^3 cryostat and calorimeter as described in Appendix I of this text.

At the lowest temperatures the accuracy of the measurement was limited by the heat capacity of the calorimeter, sample holder, etc. The heat capacity of the grease was 4.7% of the measured heat capacity at 0.4K, 9.9% at 1.0K, 46.7% at 4.0K, and 35.5% at 20K. We expect an overall accuracy in the measured heat capacity of the order of 1%.

The results above 1K are shown in Fig. 6 as C/T^3 vs T , and below 1.4K in Fig. 7 as C/T vs T^2 . The data below 0.8K suggest a weaker than T^3 temperature dependence, but the deviation from T^3 is not much greater than the uncertainty, and the accuracy is certainly not high enough to distinguish between, for example, a constant term or a linear term. Because of the uncertainty in the correct extrapolation of the data to 0K, several representations of the data have been developed. Since for our immediate applications (to the measurements on terbium ethyl sulfate) even a linear term of $0.015T$ mJ/gm-K would be negligible,

we have used only T^3 extrapolations to 0K. Table II gives smoothed values of C/T^3 from the curve through the data in Fig. 6. Equation (1) is an approximation to the data in the region 1K to 20K which has been forced to go to zero as $0.0261 T^3$.

$$C_{c,grease} = B_1 T^3 + \sum_{i=2}^9 B_i T^{b_i} \quad (1)$$

where $C_{c,grease}$ is in mJ/g-K, and

$$B_1 = 0.0261$$

$$B_2 = 9.953004 \times 10^{-5}$$

$$B_3 = -2.2604 \times 10^{-4}$$

$$B_4 = 4.45336 \times 10^{-4}$$

$$B_5 = -1.24733 \times 10^{-4}$$

$$B_6 = 1.338402 \times 10^{-5}$$

$$B_7 = -5.63988 \times 10^{-7}$$

$$B_8 = 5.02937 \times 10^{-10}$$

and $B_9 = -3.0663 \times 10^{-13}$

with $b_i = 4, 5, 6, 7, 8, 9, 11, 13.$

The deviations from Eq. (1), shown in Fig. 8, were used together with Eq. (1) in the terbium ethyl sulfate experiments. Equation (2) represents a least-squares fit to the data in which none of the coefficients were fixed.

$$C'_{c,grease} = \sum_{i=1}^8 B_i T^{b_i} \quad (2)$$

where $C'_{c,grease}$ is in mJ/g-K, and

$$B_1 = 2.80019 \times 10^{-2}$$

$$B_2 = -4.87887 \times 10^{-3}$$

$$B_3 = 3.81416 \times 10^{-3}$$

$$B_4 = -9.07297 \times 10^{-4}$$

$$B_5 = 9.76703 \times 10^{-5}$$

$$B_6 = -5.23844 \times 10^{-6}$$

$$B_7 = 1.21072 \times 10^{-7}$$

and $B_8 = -3.12038 \times 10^{-11}$

with $b_1 = 3,4,5,6,7,8,9,11.$

It represents the data between 1K and 20K to within $\pm 1\%$.

Other measurements near 1K have given a heat capacity of $0.0325T^3$ mJ/g-K for Apiezon N grease.¹⁴ The only other measurements of its heat capacity appear to be in the region above 80K.¹⁵ Measurements on Apiezon T grease have shown a similar temperature dependence, but somewhat greater in magnitude.¹⁶

APPENDIX III. THE HEAT CAPACITY OF LaCu_2

The heat capacity of LaCu_2 was measured between 0.4 and 20K to provide a basis for a crude estimate of the lattice and electronic heat capacities of PrCu_2 . Although LaCu_2 has the hexagonal AlB_2 structure which differs from that of the neighboring RECu_2 compounds which have the CeCu_2 structure,¹⁷ it is related to them by a distortion.¹⁸ It seems to provide as good a basis for comparison as would a compound with the same structure and substantially different atomic masses. The density of LaCu_2 is somewhat lower than that obtained by extrapolation in the series SmCu_2 , NdCu_2 , PrCu_2 , CeCu_2 . Its lattice heat capacity might be expected for this reason (apart from differences associated with the different structures) to be somewhat higher than that of PrCu_2 .

The results of the measurements are shown in Figs. 9 and 10 as C/T vs T^2 and $(C-\gamma T)/T^3$ vs T . The heat capacity of the LaCu_2 was 18.7% of the measured heat capacity at 0.44K, 16.7% at 1.0K, 14.2% at 5.0K, and 15.7% at 20K.

0 0 0 0 4 2 0 1 6 7 2

-21-

APPENDIX IV. DATA SHEETS

PrCu₂--Sample I

zero field

0.32 ± 20K

T(K)	C(J/mole-K)	T(K)	C(J/mole-K)
.32250	.03104	5.47811	7.84632
.34633	.02881	5.82002	8.63815
.27955	.02639	6.21655	9.49927
.41448	.02459	6.21780	9.50219
.45461	.02321	6.62112	10.22599
.50116	.02240	7.04804	10.39043
.55423	.02197	7.60474	6.75484
.61552	.02223	8.37208	4.99140
.68815	.02321	9.15549	4.77392
.75130	.02456	9.97084	4.74026
.81551	.02631	10.85784	4.80150
.88101	.02840	12.04275	5.02977
.93158	.03037	13.38498	5.43264
.99186	.03344	14.49486	5.88474
1.05401	.03712	15.63597	6.49863
1.12363	.04250	16.78428	7.17002
1.19722	.04935	17.83098	7.89218
1.27141	.05851	18.80518	8.62737
1.35776	.07256	19.69876	9.30163
1.44213	.09055		
1.51673	.11065		
1.57598	.12939		
1.66001	.16113		
1.75011	.20299		
1.85072	.25964		
1.99497	.36358		
2.16505	.51933		
2.31446	.68752		
2.45623	.87251		
2.59481	1.07562		
2.73094	1.29620		
2.90587	1.61025		
3.10635	2.00958		
3.31672	2.46622		
3.54627	2.99865		
3.80314	3.61858		
4.09848	4.35880		
4.40236	5.13321		
4.52093	5.43698		
4.72954	5.98832		
4.93064	6.50230		
5.10740	6.94520		
5.36437	7.56042		

PrCu₂--Sample II

zero field

0.06 - 0.9K

T(K)	C(J/mole-K)	T(K)	C(J/mole-K)
.06171	.34032	.26246	.04794
.06542	.29338	.28066	.04438
.06961	.26321	.28408	.04394
.07437	.23349	.29091	.04245
.07672	.21663	.31866	.03796
.07962	.20722	.31988	.03837
.08409	.18749	.32214	.03797
.08556	.18577	.35698	.03421
.09159	.16713	.35729	.03320
.09220	.16763	.36057	.03368
.09941	.15162	.39533	.03085
.09997	.14964	.39782	.03088
.10000	.14861	.41306	.02975
.10373	.14370	.44757	.02809
.10737	.13776	.46965	.02726
.10937	.13389	.50440	.02649
.10937	.13441	.52918	.02611
.11613	.12511	.56007	.02592
.11984	.11957	.58713	.02584
.11990	.11839	.61949	.02608
.12172	.11797	.68315	.02699
.12576	.11349	.73822	.02824
.13154	.10702	.79684	.03006
.13165	.10723	.85547	.03232
.13496	.10446		
.14493	.09633		
.14704	.09520		
.15940	.08610		
.16417	.08398		
.17559	.07683		
.18148	.07443		
.19368	.06843		
.20130	.06567		
.20511	.06476		
.21363	.05707		
.22384	.05795		
.22825	.05715		
.23701	.05411		
.23705	.05402		
.25154	.05058		
.25432	.04976		
.26243	.04799		

PrCu₂--Sample II

zero field

0.33 - 8.2K

T(K)	C(J/mole-K)	T(K)	C(J/mole-K)
.33038	.03706	4.79002	6.16597
.33047	.03691	5.19979	7.19637
.36582	.03334	5.63645	8.23842
.38007	.03213	6.12041	9.32461
.40792	.03014	6.57221	10.17510
.42150	.02933	6.78689	10.47669
.44871	.02807	6.82192	10.48157
.45911	.02768	6.88251	10.51320
.48836	.02685	6.91568	10.54416
.49936	.02660	6.94785	10.54072
.53297	.02605	6.98063	10.53436
.58395	.02576	7.01472	10.51006
.62957	.02602	7.05001	10.50198
.67869	.02674	7.08588	10.42044
.72621	.02781	7.12122	10.34503
.77625	.02924	7.15724	10.23777
.82653	.03097	7.19465	10.05568
.88249	.03322	7.23333	9.85779
.93188	.03552	7.26986	9.60695
1.00035	.03978	7.30757	9.18328
1.07712	.04539	7.35087	8.60778
1.16134	.05341	7.39825	7.84639
1.25246	.06499	7.45010	6.99524
1.34584	.08095	7.49973	6.39389
1.43894	.10246	7.54597	6.01208
1.52770	.12831	7.59336	5.73690
1.63774	.16785	7.64343	5.58110
1.75428	.22224	7.69506	5.47407
1.84944	.27773	7.74829	5.29309
1.86806	.29029	7.80223	5.34429
1.94701	.34632	7.85590	5.27432
2.05264	.43324	7.90955	5.22843
2.15866	.53561	7.96339	5.17485
2.27258	.66022	8.02001	5.12560
2.40630	.82919	8.07791	5.09303
2.56312	1.05338	8.13632	5.05370
2.73382	1.32975	8.21454	5.02391
2.92854	1.68174		
3.16851	2.16817		
3.43163	2.75648		
3.70371	3.40454		
4.02087	4.32845		
4.39542	5.14547		

0 0 0 0 4 2 0 1 6 7 4

-25-

PrCu₂

9 kOe

0.13 - 0.41K

T(K)	C(J/mole-K)
.13493	.42642
.14344	.38476
.15599	.33303
.16891	.29060
.18237	.25455
.19635	.22434
.21223	.19657
.23078	.17064
.25162	.14795
.27289	.12890
.29438	.11351
.31824	.10027
.34538	.08762
.37633	.07646
.41071	.06708

-26-

PrCu₂

10 kOe

0.31 - 0.64K

T(K)	C(J/Mole-K)
.31052	.12318
.32455	.11488
.34227	.10489
.36152	.09562
.38252	.08710
.40713	.07889
.43622	.07099
.47049	.06371
.51243	.05734
.56792	.05115
.63245	.04671

PrCu₂

20 kOe

0.32 - 0.62K

T(K)	C(J/Mole-K)
.32689	.33616
.34003	.31182
.35876	.28192
.37939	.25379
.40225	.22780
.42803	.20320
.45695	.18063
.48900	.16065
.52469	.14215
.56669	.12495
.61424	.10986

PrCu₂

38 kOe

0.38 - 20K

T(K)	C(J/Mole-K)	T(K)	C(J/Mole-K)
.38503	.96161	5.67776	7.68992
.40516	.87081	6.06644	8.46150
.41709	.82930	6.16589	8.65906
.43066	.77624	6.37420	8.92193
.45613	.70298	6.53904	9.12286
.47239	.65547	6.88622	9.00349
.50228	.58993	6.97889	8.77542
.52199	.54483	7.21612	8.33875
.55794	.48453	7.57766	7.18079
.58007	.44706	7.80481	6.84810
.62631	.39173	7.98938	6.53469
.65159	.36157	8.43514	6.11331
.71302	.30788	8.67499	5.93555
.73776	.28863	8.89364	5.77055
.82258	.23864	9.52051	5.51022
.82806	.23469	10.50899	5.24948
.92168	.19609	11.55456	5.40839
1.02919	.16725	12.58873	5.60442
1.15424	.14594	13.66023	5.93383
1.29283	.13572	14.67083	6.35895
1.43182	.13877	15.69470	6.89202
1.56001	.15377	16.79339	7.54326
1.67321	.17886	18.00275	8.37539
1.81410	.22652	19.26635	8.76626
1.96825	.30205		
2.11994	.40255		
2.28852	.54487		
2.45578	.72004		
2.58918	.88157		
2.74048	1.09240		
2.96489	1.44722		
3.21810	1.91127		
3.43708	2.35398		
3.64954	2.81939		
3.88243	3.35440		
4.10701	3.88360		
4.33569	4.43068		
4.66723	5.26475		
4.83029	5.68703		
5.07983	6.28454		
5.24420	6.69776		
5.50484	7.27445		

PrCu₂--Sample III

zero field

0.06 - 0.63K

T(K)	C (J/MOLE-K)
.06467	.34804
.06689	.33999
.07044	.31411
.07456	.28281
.07921	.24845
.08268	.23638
.08411	.22841
.08420	.22755
.08840	.21498
.09125	.20859
.09431	.19536
.10014	.17952
.10237	.17414
.10632	.16589
.11311	.15351
.11805	.14394
.12082	.14057
.12902	.12867
.13751	.11850
.16243	.09657
.19252	.07815
.23050	.06323
.27047	.05212
.30888	.04512
.34899	.03961
.38084	.03644
.39084	.03562
.41680	.03369
.43943	.03260
.44514	.03213
.45430	.03176
.47659	.03133
.47849	.03150
.49446	.03073
.50927	.03037
.55532	.02993
.59073	.03013
.62578	.02693

Terbium Ethyl Sulfate

zero field

0.15 - 0.5K

T(K)	C(J/mole-K)	T(K)	C(J/mole-K)
.15586	4.95004	.25163	5.98665
.16379	4.86496	.25277*	5.85503
.17165	4.92093	.25407*	5.78788
.17216	4.94367	.25550*	5.79285
.18021	5.11040	.25679*	5.61313
.18244	5.17273	.25824*	5.65516
.18729	5.32570	.25947*	5.55744
.19400	5.67030	.25982	5.62296
.19659	5.84149	.26095*	5.60011
.19994	6.03757	.26226*	5.46239
.20548	6.41513	.26386*	5.45507
.21059	6.88567	.26592*	5.43103
.21199	7.03727	.26853	5.44088
.21527	7.38391	.26857*	5.44561
.21954	7.83760	.27179*	5.32097
.22372	8.41012	.27565*	5.31249
.22512	8.01614	.28002*	5.22365
.22711	8.99411	.28486	5.05036
.23006	9.52619	.28607	5.19401
.23137 *	9.64634	.29427	5.14098
.23287	10.09355	.30555	5.03853
.23355 *	9.83556	.31458	4.95148
.23575 *	10.40855	.32491	4.87796
.23860 *	10.90512	.33538	4.79622
.23886	11.58049	.34565	4.74000
.23940 *	10.89048	.35686	4.67597
.24013 *	11.57286	.37071	4.58528
.24081 *	11.91685	.38467	4.49474
.24149 *	11.84159	.39882	4.40098
.24220 *	11.48639	.41453	4.30214
.24233	12.50060	.43109	4.21192
.24287 *	12.13046	.44851	4.11352
.24355 *	12.05652	.46528	3.99051
.24422 *	12.29138	.48385	3.87756
.24485 *	12.06581	.49874	3.78304
.24557 *	11.13633		
.24640	9.86026		
.24644 *	7.74628		
.24762 *	6.47704		
.24889 *	6.06195		
.25024 *	6.06970		
.25151 *	5.92080		

* small ΔT points

Terbium Ethyl Sulfate

zero field

0.38 - 19K

T(K)	C_M	C_L	C_{Total} (J/mole-K)
.33679	4.50044	.00038	4.50082
.40962	4.34981	.00045	4.35026
.43865	4.15673	.00055	4.15728
.47435	3.93233	.00069	3.93302
.51757	3.66590	.00090	3.66680
.52540	3.61094	.00094	3.61188
.57016	3.33084	.00120	3.33204
.57083	3.32354	.00121	3.32474
.63021	2.98903	.00162	2.99066
.63780	2.95427	.00168	2.95595
.70316	2.61408	.00226	2.61634
.71894	2.54370	.00241	2.54611
.78954	2.23126	.00319	2.23445
.80061	2.19028	.00333	2.19361
.88287	1.88172	.00447	1.88618
.88850	1.86659	.00455	1.87114
.97328	1.62623	.00598	1.63221
.99393	1.57427	.00637	1.58064
1.07484	1.38787	.00806	1.39593
1.10791	1.31951	.00883	1.32834
1.17213	1.19885	.01045	1.20930
1.22723	1.10833	.01200	1.12032
1.26011	1.06089	.01299	1.07388
1.28123	1.02893	.01365	1.04258
1.35809	.92631	.01626	.94257
1.37177	.91036	.01675	.92712
1.45816	.81182	.02012	.83194
1.50719	.76724	.02222	.78946
1.51976	.75603	.02278	.77881
1.58553	.69821	.02587	.72408
1.70131	.61287	.03196	.64483
1.72680	.59502	.03342	.62844
1.86492	.51326	.04209	.55536
1.89250	.50047	.04399	.54446
1.99813	.44734	.05177	.49911
2.14410	.38961	.06514	.45476
2.27608	.34574	.08053	.42627
2.33371	.32888	.08705	.41592
2.42791	.30385	.09351	.39736
2.56950	.27129	.11052	.38180
2.58522	.26800	.11498	.38297
2.71493	.24300	.13053	.37353
2.82341	.22469	.14593	.37062

Terbium Ethyl Sulfate--0.38 - 19K (cont.)

T(K)	C_M	C_L	C_{Total} (J/mole-K)
2.84634	.22108	.14860	.36968
3.02564	.19565	.17622	.37188
3.07439	.18950	.18728	.37678
3.18422	.17665	.20906	.38571
3.31356	.16313	.23413	.39726
3.38702	.15613	.25007	.40620
3.55422	.14179	.29059	.43237
3.57227	.14036	.29784	.43820
3.72835	.12885	.33637	.46522
3.82414	.12248	.37016	.49264
3.89260	.11821	.39038	.50859
4.03943	.10977	.44526	.55503
4.11582	.10573	.46605	.57178
4.29960	.09689	.54649	.64338
4.35153	.09459	.56481	.65940
4.47352	.08950	.62300	.71250
4.57900	.08542	.68417	.76960
4.58152	.08533	.67910	.76443
4.62017	.08391	.71576	.79967
4.82473	.07694	.82242	.89936
4.89011	.07490	.87399	.94889
4.89803	.07466	.87401	.94867
5.08158	.06936	1.00924	1.07860
5.36694	.06218	1.21782	1.28000
5.45696	.06015	1.29103	1.35118
5.75522	.05408	1.57166	1.62574
5.80697	.05312	1.61843	1.67154
6.11464	.04791	1.96116	2.00907
6.14399	.04745	2.00558	2.05303
6.58399	.04132	2.58986	2.63118
7.00680	.03648	3.19055	3.22703
7.17046	.03484	3.46111	3.49594
7.48228	.03199	3.97430	4.00629
7.70476	.03017	4.36565	4.39583
7.98536	.02809	4.93178	4.95987
8.19570	.02667	5.36150	5.38816
8.48868	.02486	6.01629	6.04115
8.66885	.02383	6.44459	6.46843
8.99075	.02216	7.15840	7.18056
9.16125	.02134	7.54686	7.56820
9.60669	.01941	8.73319	8.75260
9.81709	.01858	9.28115	9.29974
10.36856	.01666	10.77458	10.79124
10.63349	.01584	11.52208	11.53792
11.11681	.01449	13.00813	13.02262
11.41107	.01376	13.89431	13.90807
11.85104	.01275	15.24423	15.25698
12.19231	.01205	16.34611	16.35816

Terbium Ethyl Sulfate--0.38 - 19K (cont.)

T(K)	C _M	C _L	C _{Total} (J/mole-K)
12.54974	.01137	17.54393	17.55530
12.93597	.01070	18.85677	18.86747
13.28313	.01015	20.03461	20.04476
13.83058	.00936	22.09613	22.10549
14.14583	.00895	23.23497	23.24392
14.85405	.00812	25.87294	25.88106
15.18243	.00777	27.23227	27.24004
15.89815	.00709	30.15872	30.16581
16.19149	.00683	31.19554	31.20237
16.97970	.00621	34.58566	34.59187
17.18071	.00607	35.40608	35.41215
18.08877	.00547	39.36416	39.36963
18.36330	.00531	40.62545	40.63076

Terbium Ethyl Sulfate

zero field

0.38 - 20K

T(K)	C(J/Mole-K)	T(K)	C(J/Mole-K)
.38679	4.41257	2.71493	.36877
.40962	4.26497	2.82341	.36621
.43865	4.07577	2.84634	.36534
.47435	3.85592	3.02564	.36804
.51757	3.59492	3.07439	.37307
.52540	3.54108	3.18422	.38224
.57016	3.26673	3.31357	.39406
.57083	3.25958	3.38702	.40314
.63021	2.93205	3.55423	.42959
.63780	2.89803	3.57227	.43545
.70316	2.56508	3.72836	.46270
.71894	2.49624	3.82414	.49024
.78954	2.19070	3.89260	.50627
.80061	2.15066	4.03943	.55287
.88287	1.84929	4.11582	.56971
.88850	1.83454	4.29960	.64148
.97328	1.60032	4.35153	.65754
.99393	1.54977	4.47352	.71075
1.07484	1.36872	4.57901	.76792
1.10791	1.30247	4.58152	.76276
1.17213	1.18579	4.62018	.79802
1.22723	1.09859	4.82473	.89785
1.26011	1.05308	4.89011	.94742
1.28123	1.02241	4.89803	.94721
1.35809	.92441	5.08158	1.07724
1.37177	.90927	5.36694	1.27878
1.45816	.81602	5.45696	1.35000
1.50719	.77441	5.75522	1.62468
1.51976	.76399	5.80697	1.67050
1.58553	.71039	6.11464	2.00813
1.70131	.63282	6.14399	2.05210
1.72680	.61677	6.58399	2.63037
1.86492	.54529	7.00680	3.22631
1.89250	.53465	7.17046	3.49526
1.99813	.49034	7.48228	4.00566
2.09495	.49992	7.70476	4.39524
2.14410	.44712	7.98536	4.95932
2.27608	.41949	8.19571	5.38764
2.33371	.40948	8.48868	6.04066
2.42791	.39140	8.66885	6.46796
2.56950	.37648	8.99075	7.18012
2.58522	.37772	9.16125	7.56778

Terbium Ethyl Sulfate--0.38 - 20K (cont.)

T(K)	C(J/Mole-K)	T(K)	C(J/Mole-K)
9.60669	8.75222	14.14589	23.24375
9.81709	9.29937	14.85406	25.88091
10.36856	10.79092	15.18243	27.23989
10.63350	11.53761	15.89816	30.16563
11.11662	13.02234	16.19150	31.20224
11.41108	13.90781	16.97971	34.59175
11.85105	15.25673	17.18072	35.41204
12.19232	16.35793	18.08877	39.36953
12.54974	17.55508	18.36331	40.63066
12.93598	18.86727	19.19117	43.98559
13.28314	20.04457	19.64302	46.30169
13.83059	22.10531		

Apiezon N Grease

zero field

0.39 - 20K

T(K)	C(mJ/Mole-K)	T(K)	C(mJ/Mole-K)
.39228	.01522	1.14157	.03878
.41322	.00440	1.15565	.04086
.43171	.00864	1.17755	.04301
.44624	.00571	1.19371	.04672
.45939	.00681	1.23255	.06049
.47979	.00747	1.23333	.05240
.49333	.00636	1.25109	.05281
.51565	.00709	1.27411	.04899
.53275	.00602	1.30438	.05639
.54777	.00578	1.34718	.06344
.57619	.00604	1.41034	.07353
.58917	.00877	1.42036	.07131
.60248	.00716	1.45549	.07211
.60273	.00854	1.47119	.08090
.62005	.00758	1.50057	.09028
.63942	.00851	1.51417	.09743
.65329	.01102	1.53057	.09700
.65784	.00896	1.53909	.09791
.67024	.01077	1.57627	.09882
.68152	.01065	1.59511	.10887
.70323	.00912	1.61840	.11502
.72280	.01162	1.63445	.11511
.73013	.01126	1.65691	.12168
.75812	.01128	1.70108	.13451
.77283	.01351	1.78982	.15525
.79359	.01348	1.87783	.18016
.80093	.01348	1.96594	.20638
.81971	.01381	2.04999	.23518
.83611	.01572	2.15315	.27418
.85366	.01692	2.23743	.31210
.85843	.04095	2.25496	.31647
.87065	.01833	2.33949	.36057
.88882	.01952	2.38744	.38269
.89374	.01937	2.44919	.42203
.92844	.02198	2.46657	.43152
.96320	.02555	2.55042	.48099
.99078	.02699	2.67349	.56366
1.02736	.03137	2.78187	.63631
1.04104	.02940	2.88846	.70822
1.07018	.03405	2.97140	.78724
1.11437	.02787	3.03804	.84806
1.12152	.03960	3.13002	.93045

Apiezon N Grease--0.39 - 20K (cont.)

T(K)	C(mJ/Mole-K)	T(K)	C(mJ/Mole-K)
3.25373	1.05375	8.13564	14.97134
3.36594	1.17771	8.54468	16.86459
3.48688	1.32028	8.72889	17.74781
3.66450	1.54717	9.21527	20.12192
3.86239	1.82216	9.34460	20.78246
4.02544	2.07265	9.94840	24.05327
4.25796	2.44513	10.02285	24.48675
4.43766	2.78990	10.70433	28.20203
4.45837	2.84765	10.84939	29.12324
4.69936	3.31874	11.51253	33.02578
4.71207	3.37994	11.66693	33.94627
4.90526	3.82253	12.35537	38.15661
4.97413	3.94240	12.44126	38.67731
5.18927	4.48053	13.33119	44.47208
5.25376	4.60924	13.36088	44.66319
5.51416	5.33872	14.43867	51.83315
5.54053	5.40377	14.46362	52.11082
5.87362	6.37962	15.58895	59.87994
6.00456	6.81080	15.66107	60.74882
6.19962	7.41535	16.85382	69.29442
6.44293	8.27310	17.83829	77.01819
6.50329	8.45850	17.96176	78.00361
6.87823	9.82840	18.96790	85.70492
6.99848	10.27926	19.05387	86.57597
7.42586	11.87958	20.09526	94.44970
7.58412	12.54538	20.12580	94.89090
7.95269	14.12841		

LaCu₂

zero field

0.44 - 20K

T(K)	C(J/Mole-K)	T(K)	C(J/Mole-K)
.44284	.00334	1.68078	.01437
.45723	.00353	1.74861	.01519
.48296	.00364	1.97548	.01824
.50085	.00378	2.02326	.01941
.51705	.00393	2.04581	.01979
.53439	.00402	2.12741	.02115
.54005	.00403	2.14234	.02073
.55458	.00409	2.20228	.02251
.58303	.00434	2.24859	.02341
.61007	.00445	2.28005	.02358
.63583	.00470	2.29352	.02371
.64820	.00478	2.36102	.02498
.68298	.00500	2.39036	.02546
.72169	.00528	2.40966	.02624
.74579	.00548	2.44102	.02638
.74658	.00548	2.51693	.02774
.76240	.00558	2.52691	.02772
.78653	.00574	2.54612	.02874
.78737	.00567	2.59643	.02986
.80942	.00580	2.66926	.03031
.82597	.00593	2.71877	.03210
.86015	.00609	2.78460	.03351
.86465	.00620	2.85237	.03510
.89324	.00611	2.97987	.03833
.89726	.00627	3.04642	.04058
.93444	.00666	3.16730	.04361
.97098	.00696	3.26549	.04664
1.02279	.00735	3.41692	.05145
1.06052	.00799	3.54216	.05434
1.09486	.00791	3.78240	.06282
1.13072	.00771	3.91684	.06671
1.15935	.00854	4.06452	.07336
1.16225	.00862	4.23435	.08003
1.20496	.00919	4.40799	.08892
1.26930	.00993	4.59920	.09856
1.31797	.01048	4.61617	.09911
1.36893	.01054	4.83528	.11262
1.41341	.01136	4.97384	.12057
1.41872	.01128	5.07338	.12579
1.46703	.01184	5.21458	.13617
1.47910	.01197	5.23902	.13891
1.54368	.01263	5.28782	.14152

LaCu₂-0.44 - 20K (cont.)

T(K)	C(J/Mole-K)	T(K)	C(J/Mole-K)
5.59257	.16510	10.37768	1.01814
5.71462	.16930	10.50082	1.05438
5.89388	.18761	10.89062	1.18347
6.02393	.20280	11.02370	1.23818
6.11113	.20815	11.39442	1.36583
6.34436	.23030	11.54112	1.40793
6.45502	.25007	11.88066	1.54560
6.51812	.25671	12.06967	1.61736
6.76029	.28364	12.38259	1.74177
6.81726	.28825	12.99686	2.02956
7.01669	.31385	13.04716	2.03671
7.23967	.34002	13.79417	2.41651
7.27736	.34787	13.95926	2.48186
7.51436	.37860	14.52354	2.79167
7.63828	.39456	14.52938	2.80580
7.77937	.41678	15.20788	3.22393
8.02283	.45822	15.24187	3.24870
8.03808	.46092	15.91477	3.67707
8.28627	.50768	15.94056	3.69937
8.38993	.52805	16.58741	4.14162
8.57106	.56375	16.64726	4.16130
8.81972	.61290	17.35191	4.66106
8.89605	.63341	17.39889	4.70543
9.25248	.71240	18.15009	5.27061
9.31185	.72417	18.36487	5.43659
9.56500	.79359	18.96367	5.89501
9.84052	.86617	19.44492	6.30121
10.00195	.91195	19.94894	6.72020

REFERENCES

1. B. Bleaney, Proc. Roy. Soc. A276, 19 (1963).
2. T. E. Katila, private communication.
3. K. Andres, E. Bucker, J. P. Maita, and A. S. Cooper, Phys. Rev. Lett. 28(25), 1652 (1972).
4. A. H. Cooke, S. J. Swithenby and M. R. Wells, Solid State Commun. 10, 265 (1972).
5. J. H. Colwell and B. W. Mangum, Solid State Commun. 11, 83 (1972).
6. S. Hufner, Z. Physik 169, 417 (1962).
7. R. J. Anderson, J. Baker, and R. Birgeneau, J. Phys. C, 4, 1613 (1971).
8. H. Meyer and P. L. Smith, J. Phys. Chem. Solids 9, 285 (1959).
9. B. B. Triplett, Ph.D. thesis, University of California, Berkeley, 1970.
10. S. D. Bader, Ph.D. thesis, University of California, Berkeley, 1974.
11. M. M. Conway, Ph.D. thesis, University of California, Berkeley, 1972.
12. D. L. Martin, Phys. Rev. 141, 576 (1966).
13. G. Ahlers, J. Phys. Chem. Solids 28, 525 (1967).
14. Private communication from J. Scheffer, quoted by R. F. Wielinga, thesis, Leiden, Drukkerij J. H. Pasmans-'s-Gravenhage, 1968.
15. J. G. Bunting, T. Ashworth, and H. Steeple, Cryogenics 9(5), 385 (1969).
16. E. F. Westrum, Jr., Chien Chou, D. W. Osborne, and H. E. Flotow, Cryogenics 7(1), 43 (1967).

17. A. R. Storm and K. E. Benson, *Acta. Cryst.* 16, 701 (1963).
18. A. C. Larson and D. T. Cromer, *Acta. Cryst.* 14, 73 (1961).

ACKNOWLEDGEMENTS

I would like to thank Professor N. E. Phillips for his very helpful assistance and advice. I wish to express my gratitude to Sam Bader, Dr. Gary Brodale, Tracy Hall, Jr., Dr. Erwin Hornung, Brent Krusor, Gary Schwartz, and especially Bill Fogle, present and former members of this research group, for their numerous contributions.

Samples I and II of PrCu_2 and the LaCu_2 sample were prepared by Gary P. Schwartz who also collaborated on most of the measurements on those PrCu_2 samples and on their interpretation. The terbium ethyl sulfate samples were supplied by T. E. Katila who also made his susceptibility data available in advance of publication. Tom Morrison did the chemical analysis on the PrCu_2 samples.

Special thanks goes to Shirley Ashley who helped prepare the manuscript in its final form. Gloria Pelatowski prepared the illustrations.

This work was performed under the auspices of the U. S. Atomic Energy Commission.

Table I.

Terbium ethyl sulfate

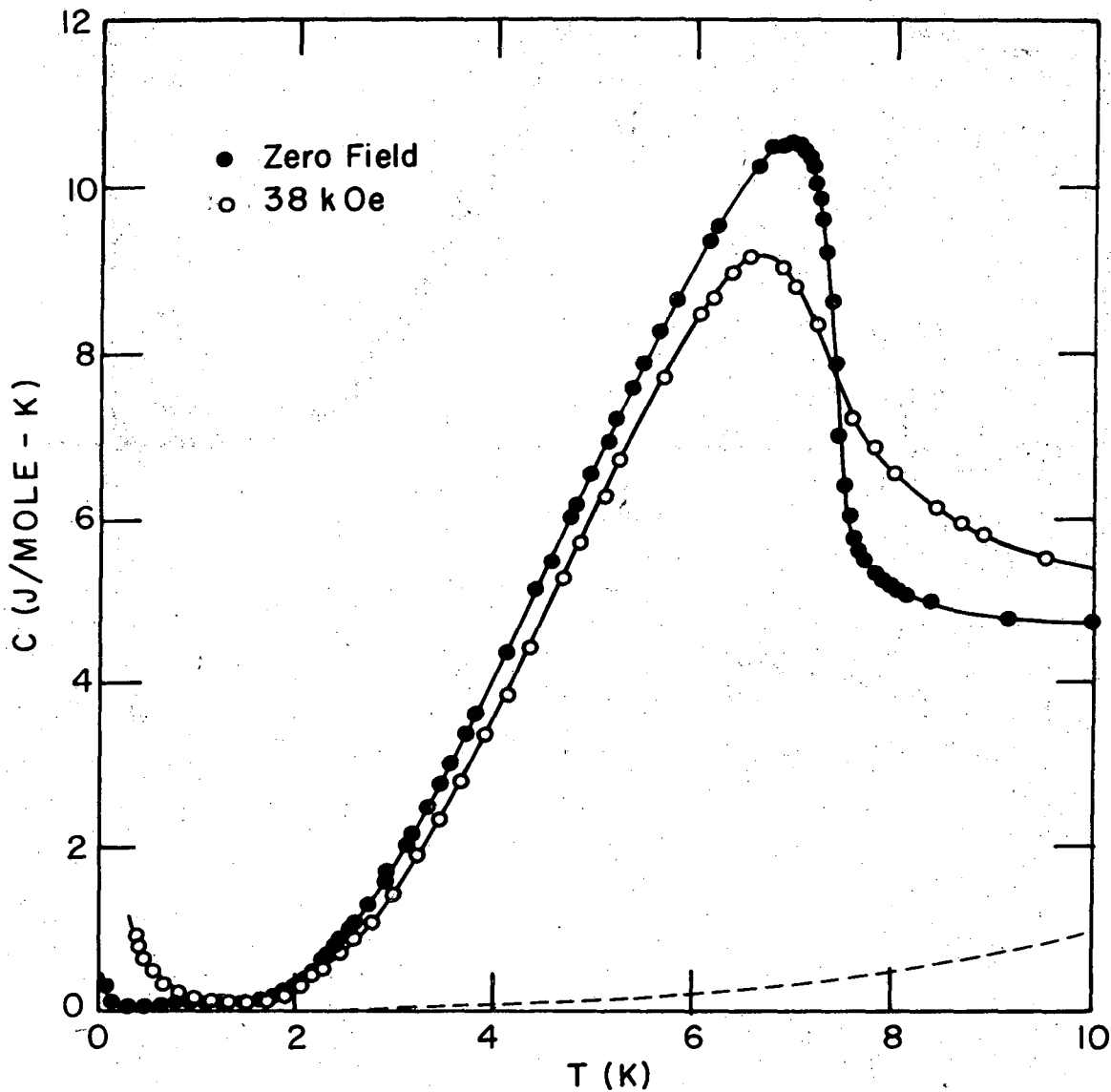
T(K)	$(C - \frac{1.79112}{T^2})/T^3$
	mJ/mole-K
2.0	6.490
3.0	6.495
4.0	6.690
5.0	7.520
6.0	8.503
7.0	9.280
8.0	9.708
9.0	9.873
10.0	9.785
11.0	9.483
12.0	9.102
13.0	8.690
14.0	8.275
15.0	7.858
16.0	7.450
17.0	7.055
18.0	6.670
19.0	6.320

Table II
Apiezon N grease

<u>T</u>	<u>C/T³ (mJ/gm-K⁴)</u>
0.5	0.02615
1.0	0.02630
1.5	0.02661
2.0	0.02741
2.5	0.02870
3.0	0.03010
3.5	0.03112
4.0	0.03182
4.5	0.03200
5.0	0.03189
6.0	0.03142
7.0	0.02990
8.0	0.02805
9.0	0.02620
10.0	0.02431
11.0	0.02244
12.0	0.02071
13.0	0.01917
14.0	0.01780
15.0	0.01652
16.0	0.01538
17.0	0.01436
18.0	0.01340
19.0	0.01250
20.0	0.01169

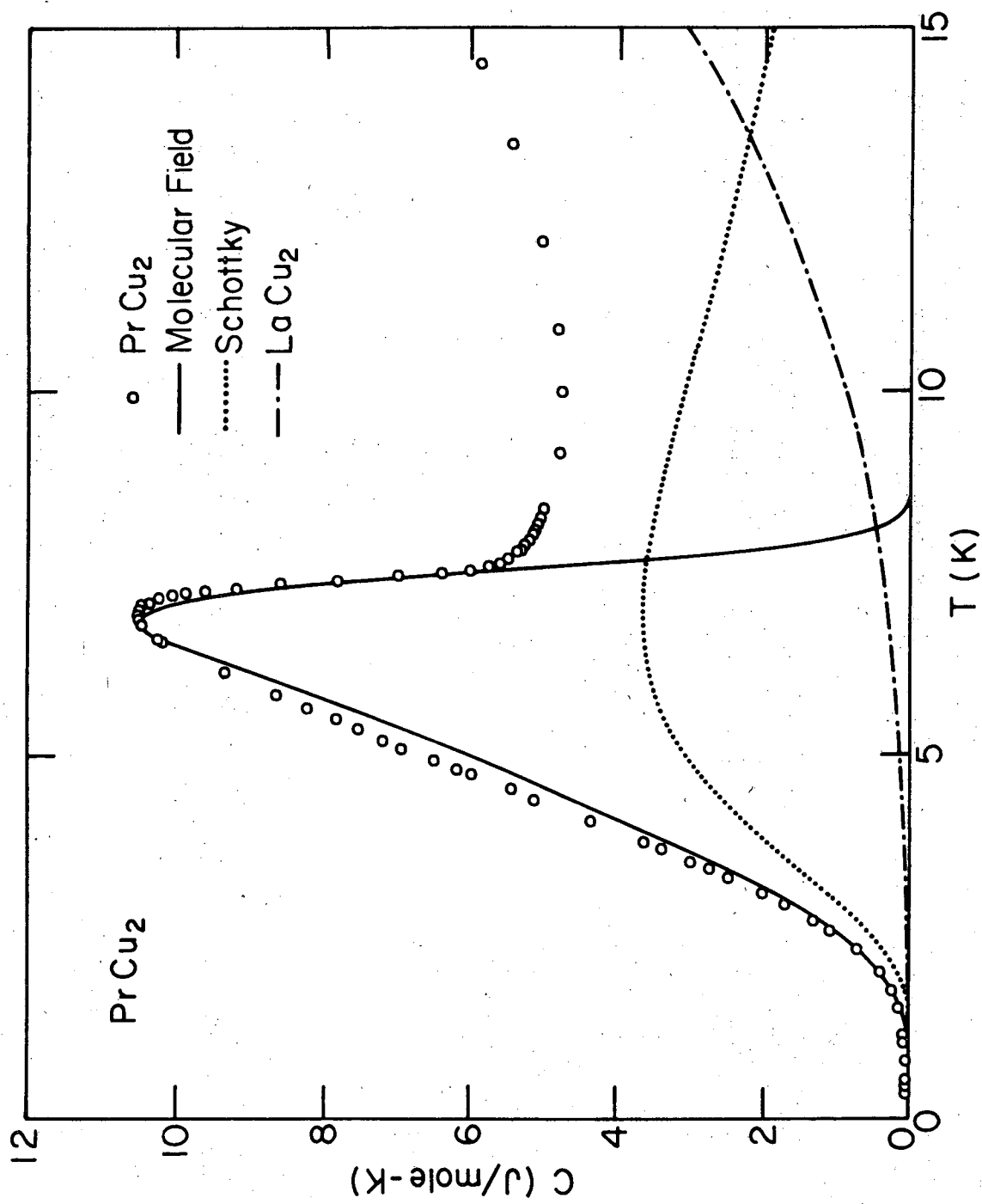
FIGURE CAPTIONS

- Fig. 1. The heat capacity of PrCu_2 in zero field and in 38 kOe. The dashed curve represents the heat capacity of LaCu_2 .
- Fig. 2. The heat capacity of PrCu_2 in zero magnetic field compared with a molecular field calculation for a Jahn-Teller distortion and with a Schottky anomaly.
- Fig. 3. Low temperature data on PrCu_2 in several magnetic fields.
- Fig. 4. The magnetic heat capacity of terbium ethyl sulfate.
- Fig. 5. The lattice heat capacity of terbium ethyl sulfate.
- Fig. 6. The heat capacity of Apiezon-N grease.
- Fig. 7. The heat capacity of Apiezon-N grease.
- Fig. 8. Deviation of the heat capacity of Apiezon-N grease from the equation given in the text.
- Fig. 9. The heat capacity of LaCu_2 .
- Fig. 10. The lattice heat capacity of LaCu_2 .



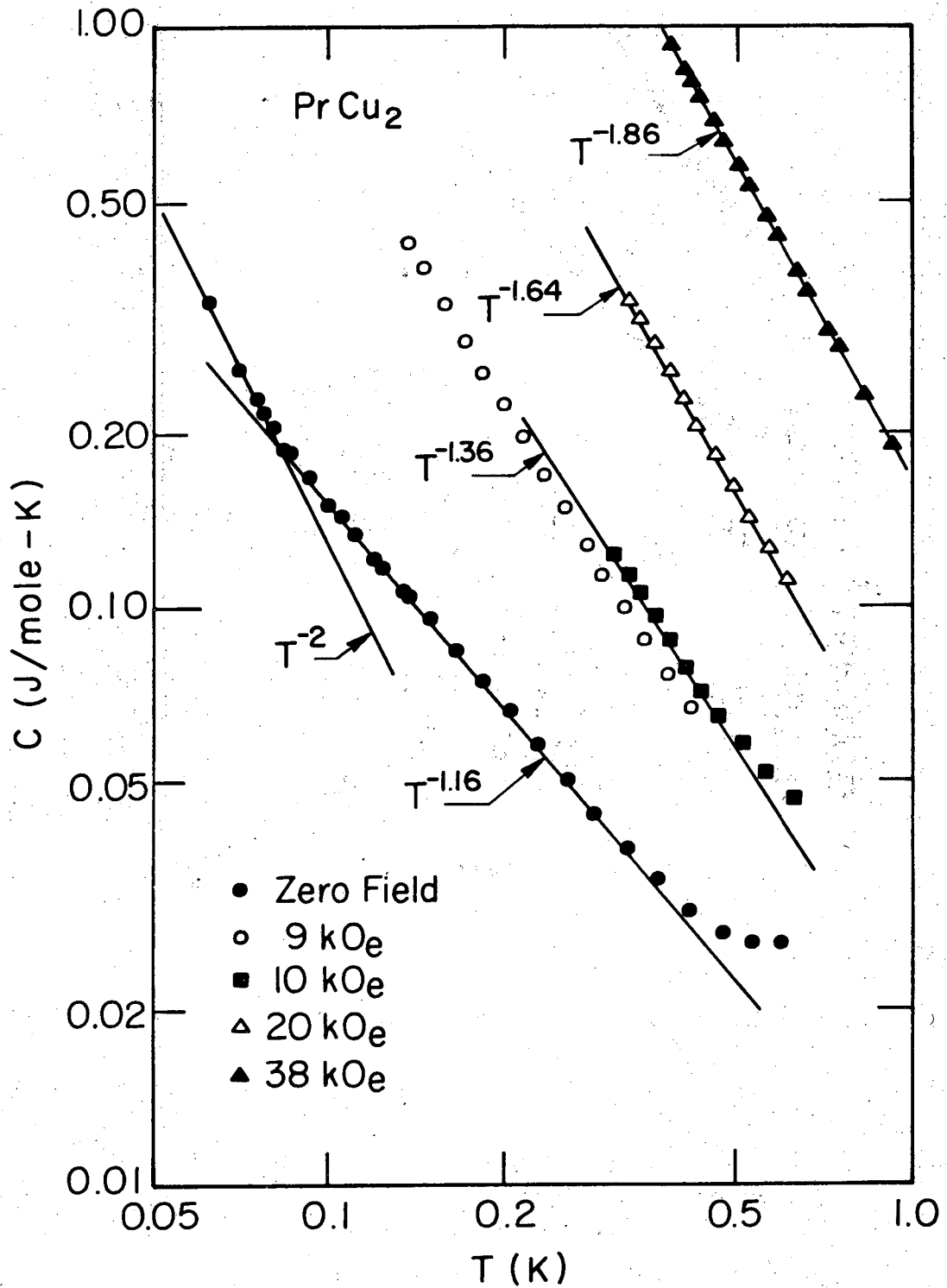
XBL 741-5467

Fig. 1



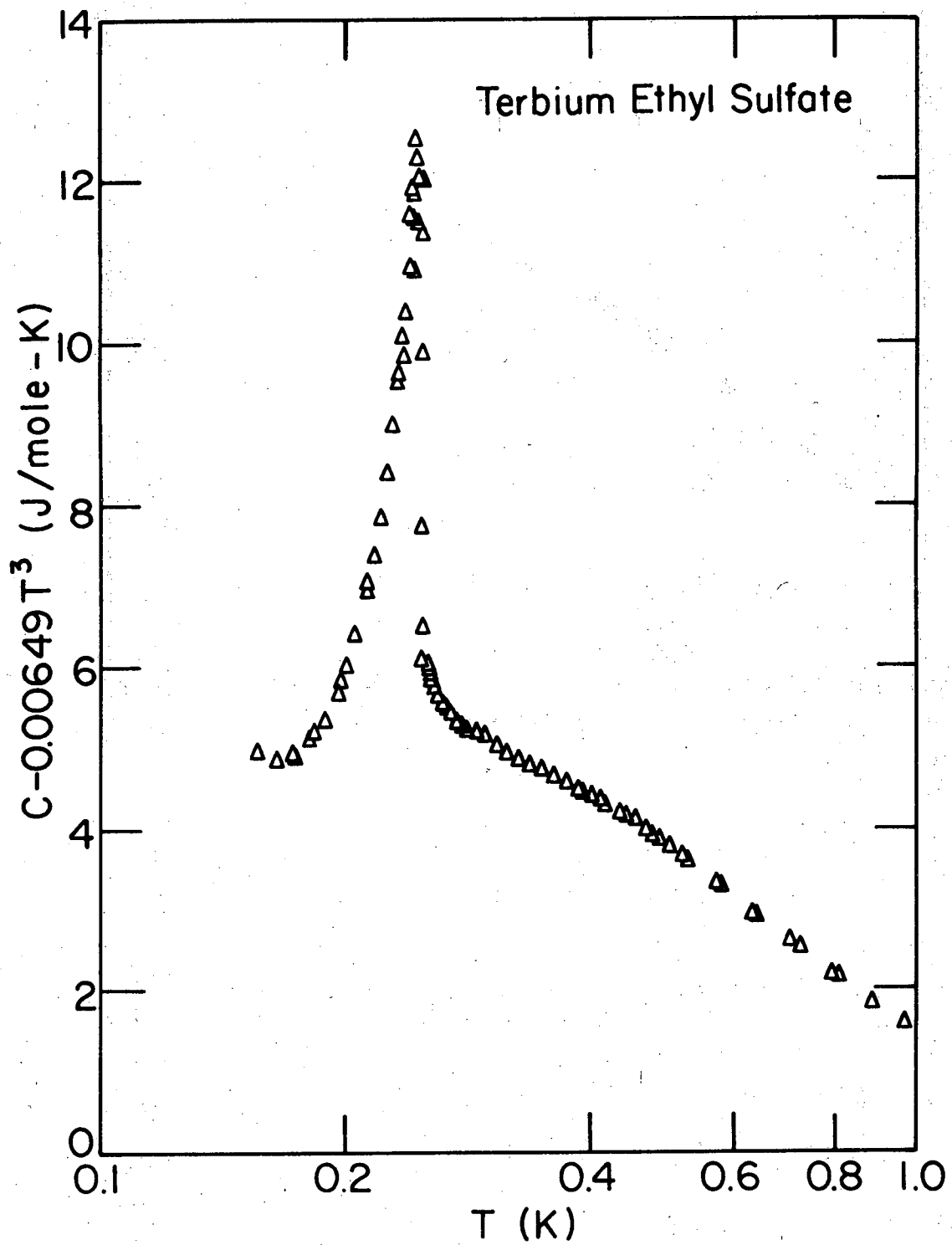
XBL 749-7270

Fig. 2



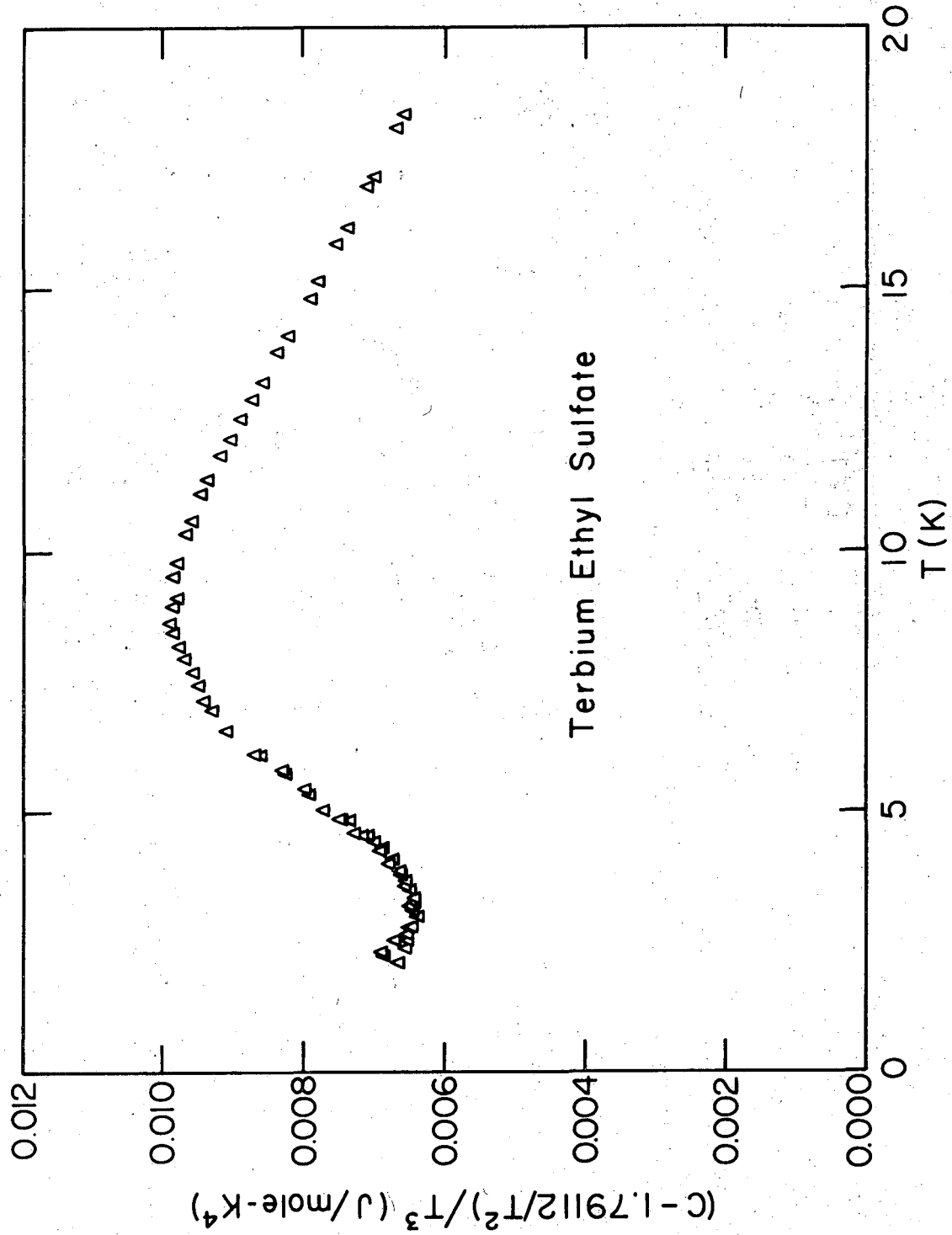
XBL 749-7270

Fig. 3



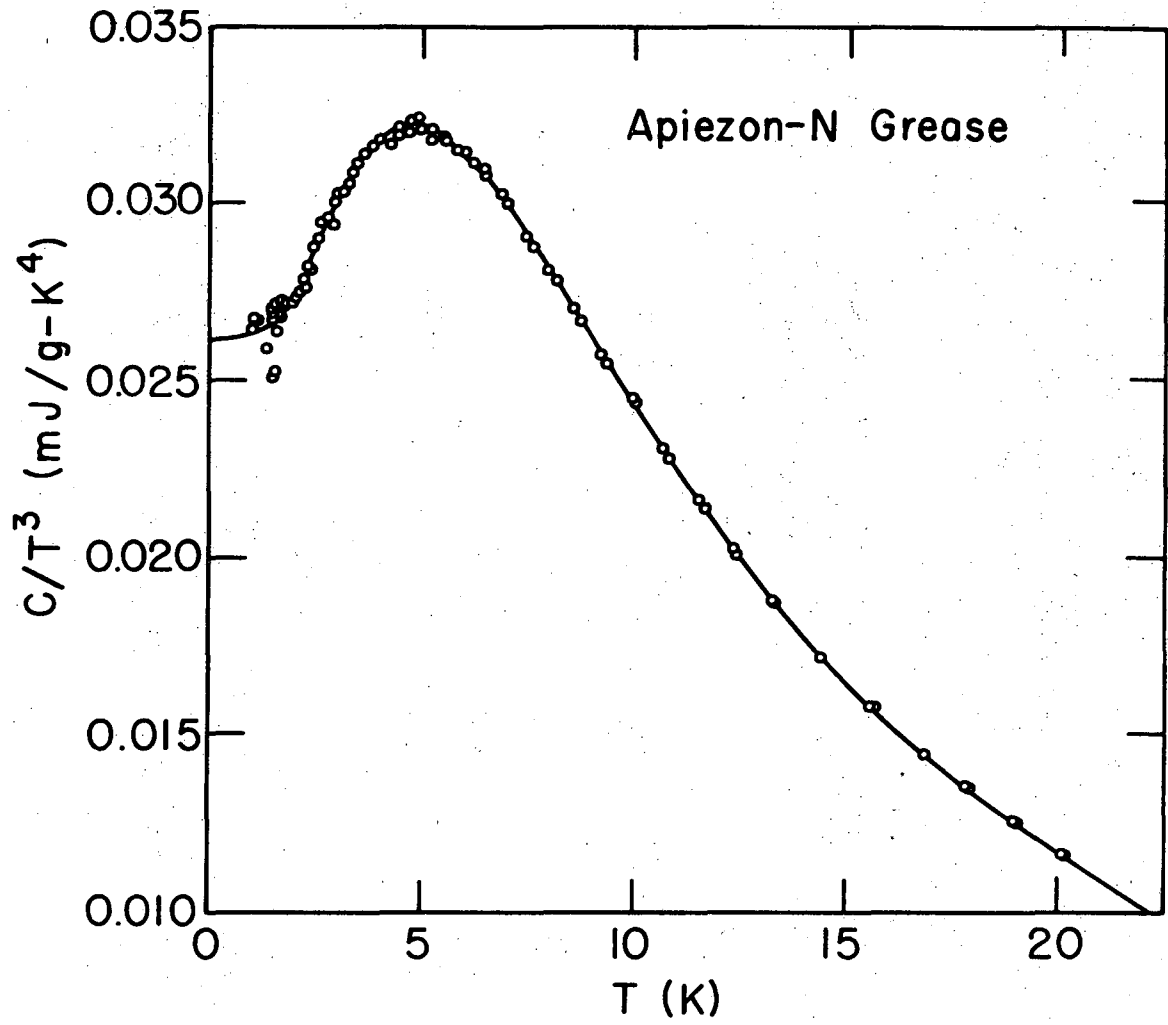
XBL 749-7274

Fig. 4



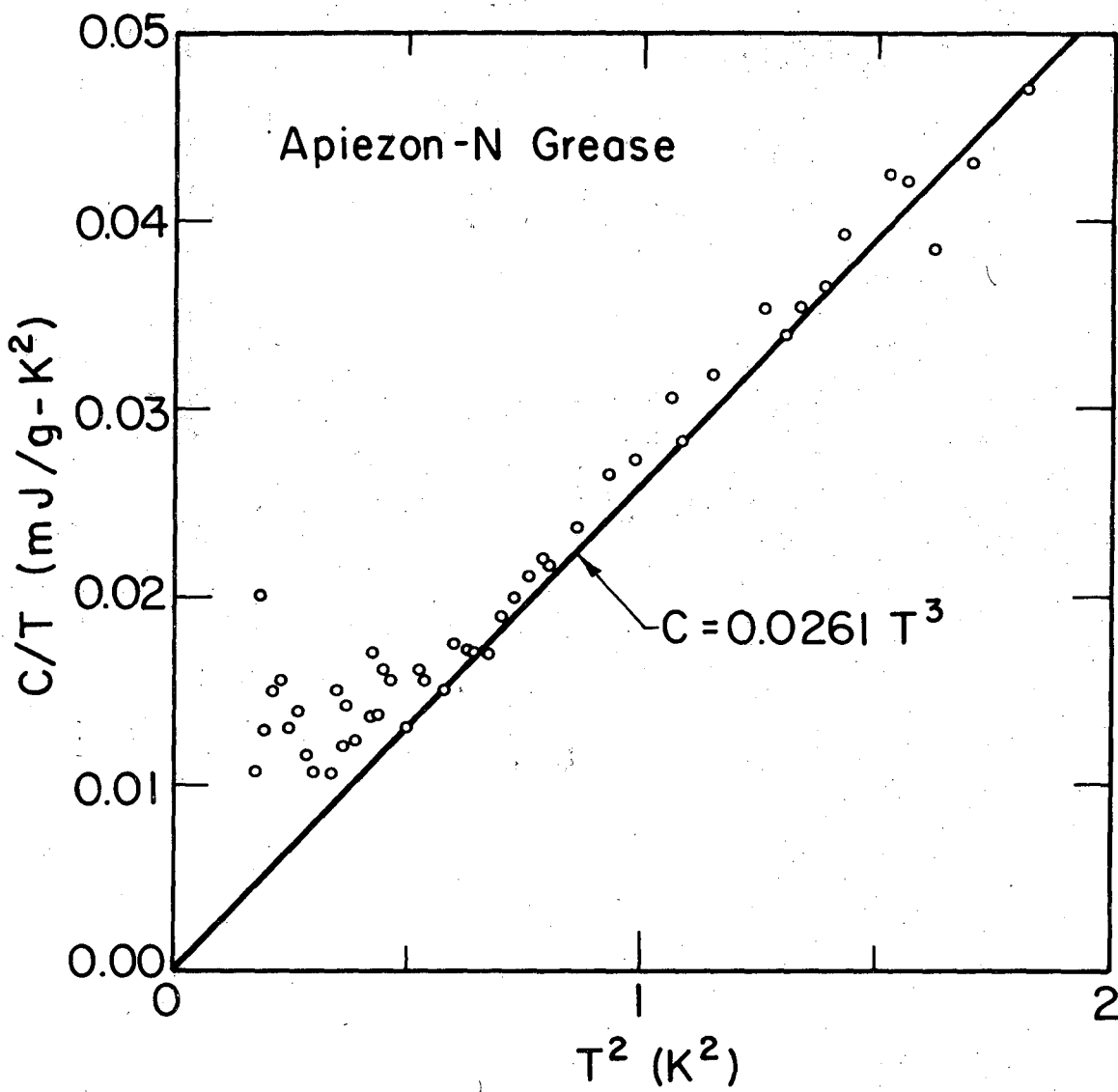
XBL 749-7268

Fig. 5



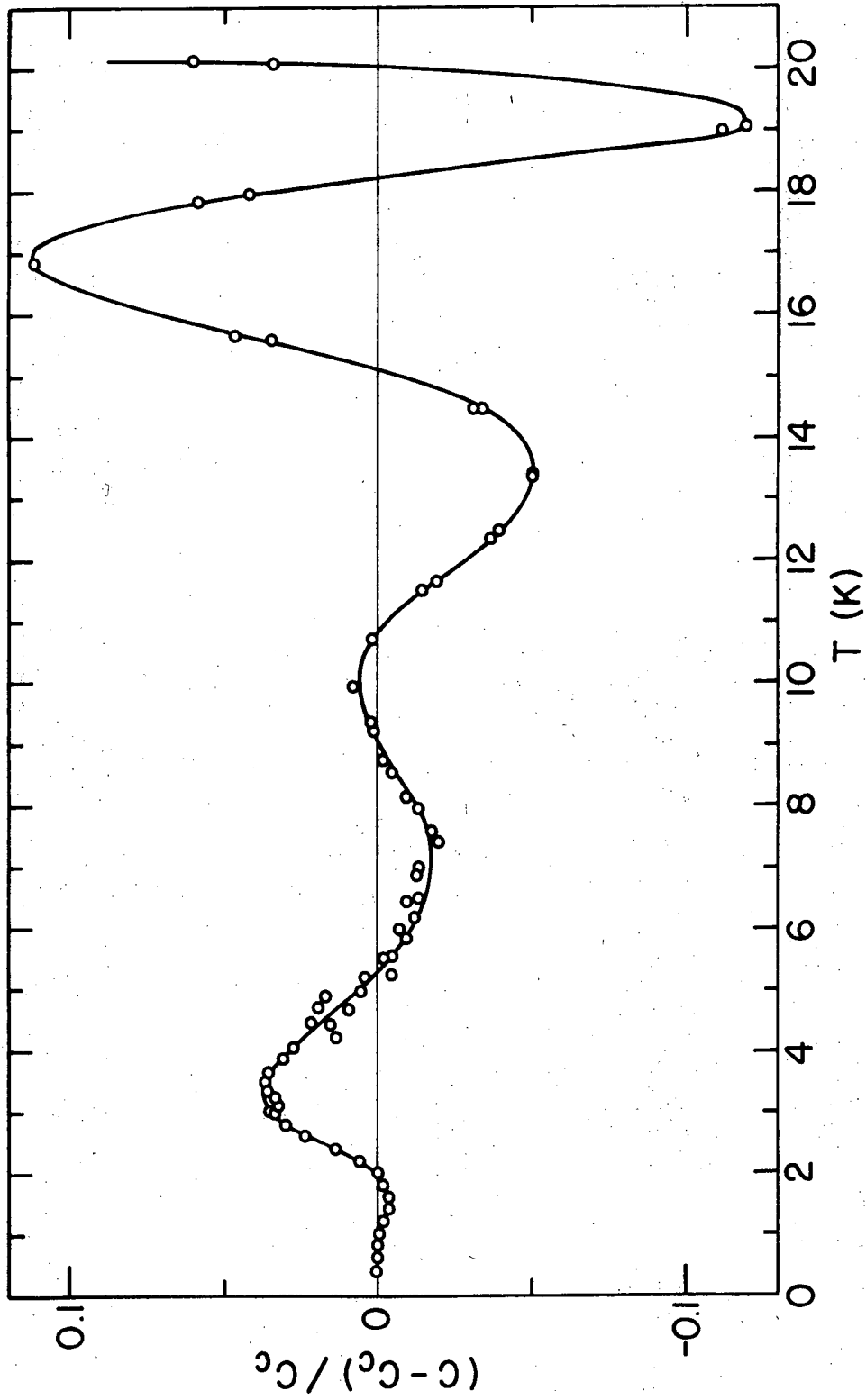
XBL 749-7267

Fig. 6



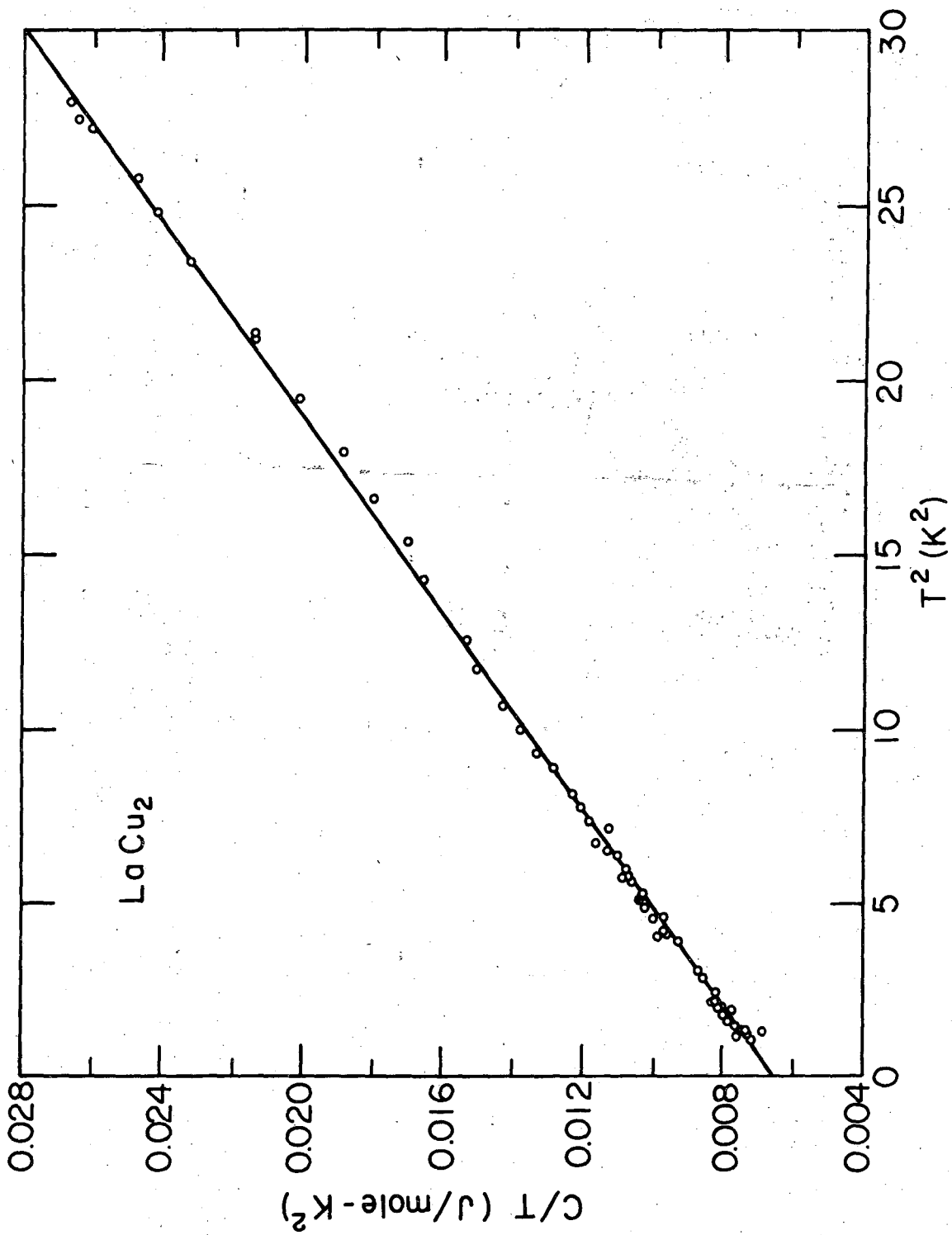
XBL 749-7273

Fig. 7



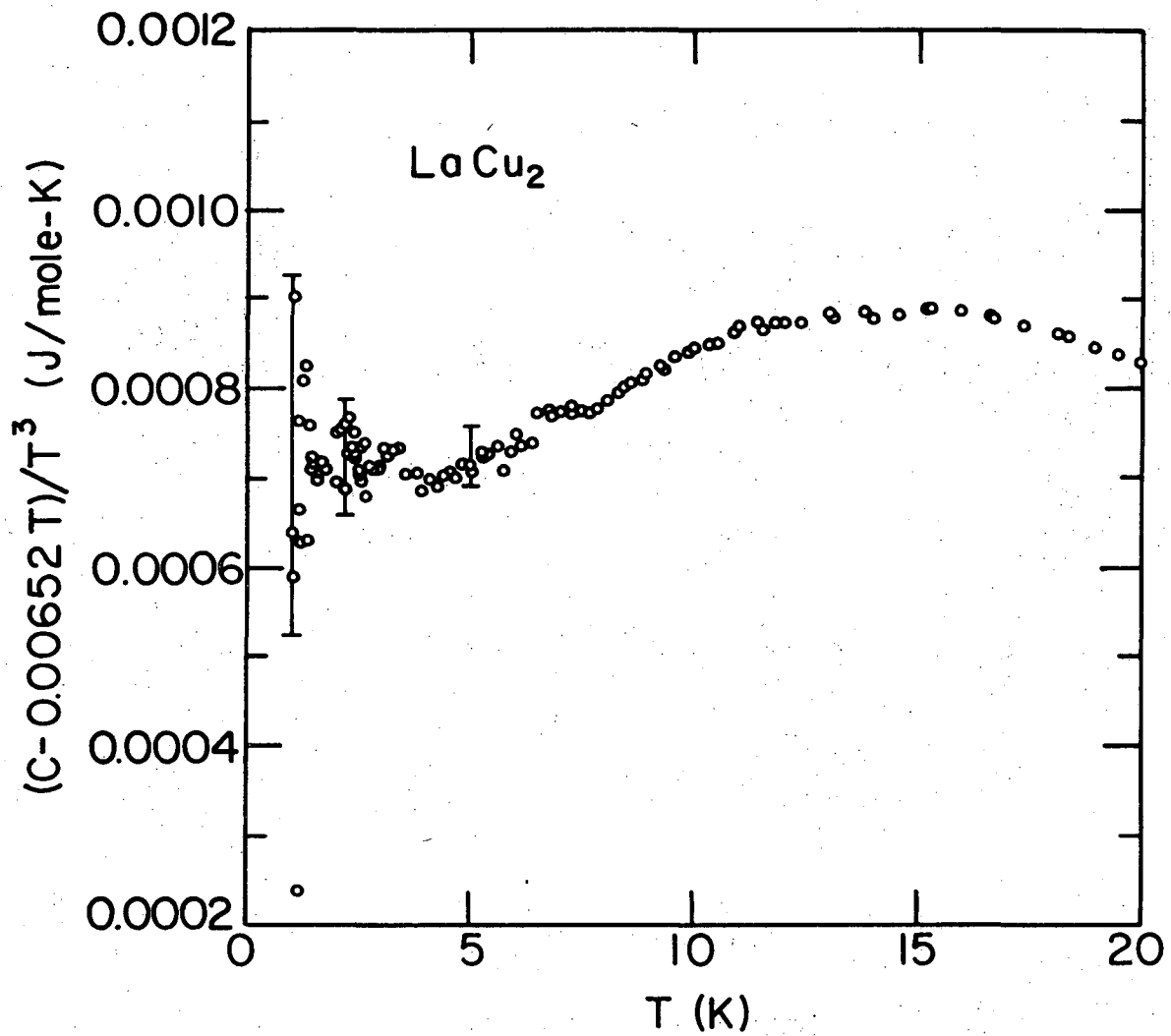
XBL 749-7269

Fig. 8



XBL 749-7272

Fig. 9



XBL 749-7271

Fig. 10

LEGAL NOTICE

This report was prepared as an account of work sponsored by the United States Government. Neither the United States nor the United States Atomic Energy Commission, nor any of their employees, nor any of their contractors, subcontractors, or their employees, makes any warranty, express or implied, or assumes any legal liability or responsibility for the accuracy, completeness or usefulness of any information, apparatus, product or process disclosed, or represents that its use would not infringe privately owned rights.

TECHNICAL INFORMATION DIVISION
LAWRENCE BERKELEY LABORATORY
UNIVERSITY OF CALIFORNIA
BERKELEY, CALIFORNIA 94720